Femtosecond Pump/Probe Spectroscopy of CO on Ru{10$\bar{1}$0} from Experimental and Theoretical Perspectives†

Jonathan P. R. Symonds, Heike Arnolds,* and David A. King

Department of Chemistry, University of Cambridge, Lensfield Road, Cambridge CB2 1EW, United Kingdom

Received: January 22, 2004; In Final Form: March 5, 2004

The effect of an 800 nm pump pulse on the C−O vibrational stretch of carbon monoxide adsorbed on Ru{10$\bar{1}$0} is followed in real time with vis−IR sum frequency spectroscopy. The observed transient red shift can be modeled by the thermal effect of the laser, acting upon one of the adsorbate phonon modes. We find that the temperature of the mode could couple to the substrate electron heat bath with a time constant of 5−10 ps, while also assuming coupling to the lattice heat bath. We also consider the effect of the degree of electronic coupling (and other rapid effects) upon the theoretical form of such spectra, and from this conclude that the observed red shift in this case must indeed be due to thermal effects.

Introduction

Ultrafast pulsed lasers have been used for two decades to investigate surface dynamics on the picosecond to subpicosecond time scales. Such lasers offer a means of distinguishing between the influence of electrons and phonons upon vibrational dynamics. They provide a means to separate the excitation and detection processes with a variable time delay in the form of *pump/probe* spectroscopy.

In this paper we investigate the influence of surface structure upon the vibrational dynamics of carbon monoxide on ruthenium using femtosecond visible pump/sum frequency probe spectroscopy. The surface chosen for study was the {10$\bar{1}$0} plane, which is ridged (open) in nature, and upon which CO forms a wide variety of structures with increasing coverage.[1,2] We compare our data with those of Bonn[3] for CO on the close-packed {0001} surface. We also predict the form of such spectra in the limit of the fastest possible processes, e.g., direct electronic excitation.

The simplest vibrational mode to be studied in surface science, and hence the most widely studied, is without doubt the C−O stretch due to its large dynamic dipole moment. If the C−O stretch is directly excited with a mid-IR pump pulse, then the absorption of a mid-IR probe pulse will allow the vibrational population decay (T_1) to be monitored, as demonstrated by Beckerle.[4]

The C−O stretch has also been indirectly excited by heating the surface− adsorbate system with short laser pulses.[5,6] From static temperature-dependent measurements of the C−O stretch it has been deduced in the past[7] that the observed frequency shift and increase in line width are due to anharmonic coupling between the high-frequency C−O stretch and low-frequency adsorbate phonon modes such as the frustrated translation or rotation. An increase in temperature increases the population of these low-frequency modes, which in turn affects the frequency and line width of the C−O stretch. The extent of any frequency shift and line width change is determined by the degree of anharmonic coupling and the frequency of the phonon mode and its damping rate.[8] If the phonon mode frequency lies below the Debye frequency of the solid, coupling to both electronic and lattice heat baths is possible.

However, during steady-state temperature dependence measurements, the electrons and phonons of the solid are in equilibrium, and therefore, it is difficult to distinguish between the prevalent damping mechanisms, electron−hole pair excitation and relaxation via phonons.[9] Ultrafast pulsed lasers provide a means to see beyond the equilibrium picture so that an attempt can be made to distinguish between these mechanisms. When such a laser pulse heats a surface, initially the temperature of the electron bath alone increases due to its small heat capacity, followed by equilibration of the lattice heat bath on a picosecond time scale. Thus, one has a time interval of typically 1−10 ps, depending upon the degree of electron−lattice thermal coupling, to attempt to distinguish between thermal electron and lattice damping processes.

The first time-resolved experiments were conducted on CO on Pt{111},[10] Cu{111},[6] and Cu{100}.[5] The results can be summarized in terms of the coupling constants and the vibrational mode to the electron and lattice heat baths. On copper, after excitation with a visible laser pulse, values of τ_{el} = 6 ps/5.1 ps and τ_{lat} = 7 ps/4.2 ps were found for the {111} and {100} surfaces, respectively. On Pt{111}, with 20 times stronger electron−phonon thermal coupling it was only possible to assume exclusive coupling either to the electrons (τ_{el} = 2 ps) or to the lattice (τ_{lat} < 1 ps).

Sum-frequency generation (SFG) is a highly sensitive, surface-specific detection technique ideally suited to high-powered laser spectroscopic applications in the field of surface science.[11] In a medium without inversion symmetry (such as at a surface or interface) two high-intensity laser pulses may undergo a second-order nonlinear optical process, producing light at the sum of their frequencies. For vibrational experiments, IR and visible (vis) beams are used, such that the IR beam excites an adsorbed molecule to its first (or higher) vibrational level. The vis beam *upconverts* the energy to a virtual electronic state, the resulting optical decay from which is detected in the visible region of the spectrum. All IR spectral features remain, but with the signal enhanced by the mere presence of the substrate.

Recently, near-IR excitation of CO/Ru{0001} was monitored[3] with femtosecond SFG up to fluences high enough to cause desorption. The change in C−O frequency under low fluence conditions could be modeled using coupling of the frustrated translational phonon mode to the lattice with τ_{lat} = 1 ps, as deduced from desorption measurements.[12] For fluences high

† Part of the special issue "Gerhard Ertl Festschrift".

* To whom correspondence should be addressed. E-mail: ha209@cam.ac.uk.

10.1021/jp049679+ CCC: $27.50
Published on Web 05/15/2004

enough to cause desorption, coupling to other modes such as the frustrated rotation had to be additionally included.

We performed similar near-IR pump/SFG probe measurements for CO adsorbed on the more open surface, but at a low fluence comparable to that used in the study by Bonn et al.[3] At our absorbed pump fluence of 24 J m^{-2} we calculate a lattice temperature rise from 100 K to maximally 260 K. Over this temperature range we compare the transient red shift with new static temperature-dependent SF measurements of the C−O stretch frequency.

Unlike the close-packed surface,[3,13] we cannot exclude the need to include coupling of the low-frequency mode to the electronic heat bath but can place limits on τ_{el} and τ_{lat}. In addition we discuss the effect very rapid (<200 fs) changes in the C−O frequency would have upon the form of pump/probe sum-frequency spectra.

Experimental Method and Results

Full details of the broad-band/femtosecond sum-frequency spectrometer are published elsewhere.[14,15] In brief, a Spectra Physics Tsunami 90 fs oscillator delivers 800 nm nanojoule pulses to a 10 Hz regenerative amplifier. The amplifier produces 140 fs pulses at 5 mJ of energy per pulse. A Light Conversion TOPAS optical parametric amplifier is pumped by 2 mJ of this to produce mid-infrared (IR) pulses from 3 to 10 μm at energies of around 10 μJ. The remainder of the 800 nm beam is passed through a self-built pulse shaper to produce the narrow-band vis pulses used for SFG upconversion. The vis and IR beams pass onto a custom-built optical table mounted around the ultra-high-vacuum (UHV) chamber and through a single CaF_2 lens of 25 cm focal length before entering the chamber. A novel technique using a layer of temporarily adsorbed alkali metal on the single-crystal sample to generate a large nonresonant SF signal allows rapid spatial and temporal alignment of vis and IR beams on the surface. This also provides a means to cross-correlate the beams in vacuo and thus provide reliable characterization of the lasers in situ.[14] The IR beam enters at 84° to the surface normal, and the vis beam at 80°. Spectral calibration is via a chemical cell containing 10 mmol of $W(CO)_6$ in CCl_4 temporarily inserted in the IR beam path. The SF signal emerges on reflection at 81° to the surface normal and is detected by an Andor i-Star intensified charged-coupled device (ICCD) attached to an Acton 0.3 m imaging spectrograph. The UHV system is equipped with Getter sources for alkali-metal deposition, a quadrupole mass spectrometer, ion sputter gun, and Auger electron spectroscopy/low-energy electron diffraction (AES/LEED) apparatus. The base pressure is 10^{-10} mbar.

Details of the sample preparation are given elsewhere[15] but consisted of argon ion bombardment, heating in oxygen and annealing at up to 1450 K. Surface cleanliness was determined by AES and temperature-programmed desorption (TPD), and surface order by LEED. A full coverage dependence of the CO stretch measured by broad-band SFG, along with temporally resolved free induction decays and a comparison with line width, was also performed.[15]

The visible pump beam is the "waste" 800 nm light not used by the OPA, deflected by a dichroic mirror. This is filtered with six narrow-band dielectric mirrors, and passed via a computer-controlled translation stage and a 3 m focal length lens through the CaF_2 lens and into the chamber. The pump beam almost exactly follows the path of the IR beam, but emerges at a slightly raised angle in the vertical plane to avoid any possibility of entry into the detector. The pump energy was 250 μJ, and from the beam overlap, given 40% measured reflectivity from the surface, we estimate the absorbed fluence of the pump beam to be 24 J m^{-2}. Using the adsorbed alkali-metal layer method mentioned above, exhaustive checks for nonchemical effects on the vis−IR SF spectral profile caused by the presence of the pump beam were made, and none were observed. Time zero was determined by observing the pump-IR SF signal on the alkali-metal layer.

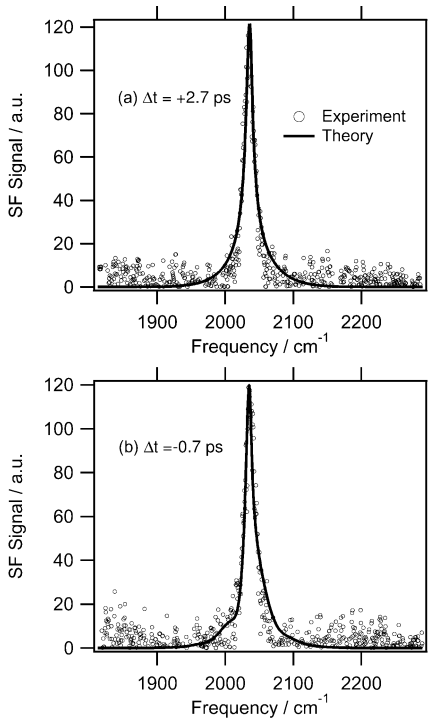

Figure 1. Example experimental and theoretical pump/probe spectra for (a) a pump pulse arriving before probe pulses and (b) a pump pulse arriving after probe pulses. For the theoretical curves, $\tau_{el} = \tau_{lat} = 1$ ps.

CO was adsorbed at 100 K, up to a coverage of 0.9 monolayer (ML), determined by TPD (1.22 ML is the saturation coverage for CO/Ru{10$\bar{1}$0}[1,2]). Ten SF spectra were taken for various pump/probe delays, Δt, at 10^4 laser shots per spectrum. Throughout this paper, $\Delta t < 0$ refers to the pump arriving *after* the probe. Examples of these spectra are given in Figure 1.

The total second-order susceptibility $\chi^{(2)}$ in a surface SFG process is conventionally written as[16]

$$\chi^{(2)} = A_0 e^{i\phi} + \sum_n \frac{A_n}{\omega_{IR} - \omega_n + i\Gamma_n} \qquad (1)$$

where A_0 and ϕ are the magnitude and phase of the nonresonant contribution and A_n, ω_n, and Γ_n are the amplitude, frequency, and half-width of the resonance. However, the nonresonant signal from the Ru{10$\bar{1}$0} surface is negligible at just 5 counts over 10^4 laser shots. Given that the SF signal is proportional to $|\chi^{(2)}|^2$, the SF spectra from CO on Ru{10$\bar{1}$0} are fitted to a simple Lorentzian function to find the center frequency and width. The center frequencies are plotted in Figure 2. We observe a maximum frequency shift of 4 cm^{-1}. In practice, upconversion with a vis pulse of finite Gaussian spectral width will produce a Voigt line shape,[15] but this is hardly discernible for these data. We shall see later that, for pump/probe spectra, even this may prove to be an oversimplification, due to the influence of the pump beam.

To determine the static temperature dependence of the C−O stretch, SF spectra were taken for various sample temperatures at $\Theta = 0.9$ ML, and these are shown in Figure 3. Each spectrum was accumulated for 10^4 laser shots, in the same manner as that discussed in our previous publication on this surface.[15] Over this temperature range, the change in stretch frequency is

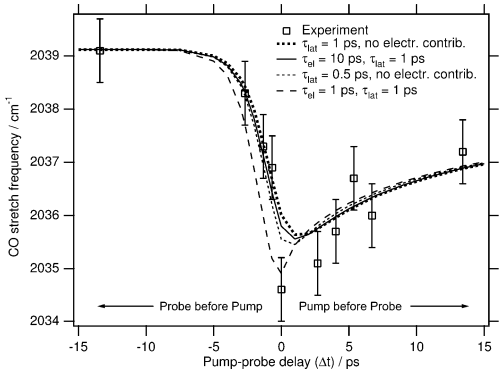

Figure 2. Center frequency of the C−O stretch as a function of pump/probe delay for both experiment and theory.

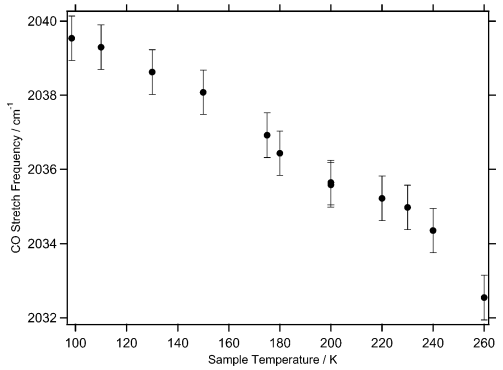

Figure 3. Experimentally determined C−O stretch frequency as a function of sample temperature, at 0.9 ML coverage.

approximately linear, corresponding to $d\nu/dT = -0.043$ cm^{-1} K^{-1}. No change within experimental error was seen in the line width over this temperature range.

Theoretical Modeling

As explained in the Introduction, previous studies[3,5,6] have indicated that such an observed frequency shift due to a visible pump laser is caused by laser-induced heating. To test to what extent this is the case for our system, the following methodology was applied. First, the relationship between sample temperature and CO stretch frequency was experimentally determined, as described in the previous section. Then, the heating effect upon the adsorbate layer of the pump laser was calculated using a two-temperature model. Finally, the SF spectra were modeled using a density matrix formalism and checked against the experimental data.

The modeling of the laser-induced adsorbate heating is based upon the two-temperature model proposed by Anisimov[17] and extended by others,[10] used extensively in the literature. This involved numerically solving[18] the following coupled differential equations:

$$C_e \frac{\partial T_e}{\partial t} = \kappa \nabla^2 T_e + g(T_l - T_e) + S(z,t) \quad (2)$$

$$C_l \frac{\partial T_l}{\partial t} = -g(T_l - T_e) \quad (3)$$

$$C_a \frac{\partial T_a}{\partial t} = -g_e(T_a - T_e) - g_l(T_a - T_l) \quad (4)$$

where T_e, T_l, and T_a are the electronic, lattice, and adsorbate temperatures, g, g_l, and g_e are the electron−lattice, adsorbate−lattice, and adsorbate−electron coupling constants, κ is the thermal conductivity, C_l is the lattice heat capacity, and C_e is the electronic heat capacity, assumed to be of the form $C_e = \gamma T_e$, where γ is a constant. $S(z,t)$ is the laser source term given by

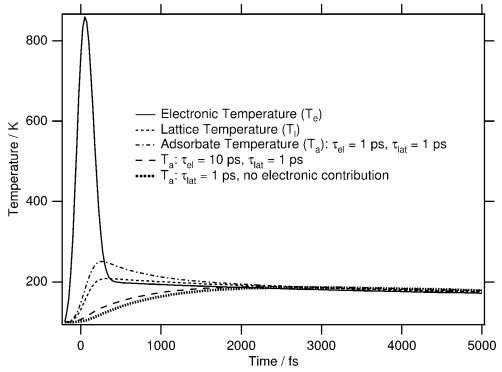

Figure 4. Model of electronic, lattice, and adsorbate temperatures of CO/Ru{10$\bar{1}$0} after an incident 800 nm laser pulse, 24 J m^{-2} of which is absorbed.

$$S(z,t) = 2I(t)(1 - R)\frac{\exp(-2z/\delta)}{\delta} \quad (5)$$

where $I(t)$ is the laser intensity as a function of time, R is the substrate reflectivity, z is the depth of the substrate, and δ is the optical skin depth. In terms of the coupling constants referred to in the Introduction, $C_a/g_e = \tau_{el}$ and $C_a/g_l = \tau_{lat}$.

The simulation was performed for various values of the thermal coupling constants to the electrons and phonons, τ_{el} and τ_{lat}, and the pump laser parameters as given above. Other physical coefficients were determined from material data sheets and from Funk et al.[12] The results are shown as Figure 4. An estimate of the frequency change caused by the pump laser is then simply given by

$$\Omega(\Delta t) = \left(\frac{d\nu}{dT}\right) T_a(\Delta t) + \text{const} \quad (6)$$

In fact this directly fits the data quite well for $\Delta t > 0$, but does not model the coherent interaction responsible for the noticeable frequency shift at $\Delta t < 0$. It also overestimates the magnitude of the frequency shift. To more properly model the SF spectra, a density matrix method was used.

The polarization set up by an infrared field in time, $P(t)$, can be determined from the density matrix, $\rho(t)$, of the two-level (a, b) system as

$$P(t) \propto \text{tr}[\hat{\rho}(t)\hat{\mu}] \quad (7)$$

where $\hat{\mu}$ is the electric dipole operator in matrix form.[16] The infrared spectrum from such a polarization is simply given by its Fourier transform. For an SF process it is possible to convolve the electric field of the vis pulse during the transform to obtain the exact SF spectra; however, as the experimental spectra described herein have already been calibrated over the true IR frequency range, this step was deemed unnecessary.

The near-resonance time evolution of the density matrix driven by an infrared electric field is best described by the optical Bloch equations[19]

$$\frac{du}{dt} = \Omega(t - \Delta t)v - \frac{u}{T_2} \quad (8)$$

$$\frac{dv}{dt} = -\Omega(t - \Delta t)u - \frac{v}{T_2} + \kappa E_{IR}(t)w \quad (9)$$

$$\frac{dw}{dt} = -\frac{w - w_{eq}}{T_1} - \kappa E_{IR}(t)v \quad (10)$$

such that $\rho_{ba} = u + iv$, $\rho_{ab} = u - iv$, and $w = \rho_{bb} - \rho_{aa}$ (the population difference). The CO stretch frequency, $\Omega(t)$, is obtained from eq 6 as described above. The temporal form of the IR electric field, $E_{IR}(t)$, is obtained from the alkali-metal in situ cross-correlation technique.[14] The total dephasing time, T_2, has been measured by us using a free induction decay experiment[15] to be 1.22 ps at $\Theta = 0.89$ ML; it is deemed not to be a function of time as the empirical sample temperature-dependent spectra showed no real variation in line width with temperature. The resonance lifetime, T_1, is estimated to be 3 ps, but in practice this seems to have little effect on the simulation. The field coupling constant, κ, is estimated to be $2D/\hbar$; however, this largely affects just the amplitude of the spectra within a range of reasonable values.

Equations 8−10 were solved for each value of Δt using a fourth-order Runge−Kutta method with an adaptive step size. The initial values were $u_0 = v_0 = 0$ and $w_0 = w_{eq} = -1$. Given that the on-diagonal elements of $\hat{\mu}$ are zero, and the off-diagonal elements are mutually conjugate, it follows from eq 7 that $P(t) \propto u(t) - v(t)$. A fast Fourier transform routine was applied to each temporal polarization to obtain each spectrum.

Two examples of the spectra obtained are shown in Figure 1 with their corresponding experimental spectra. The side peak at lower frequency in the $\Delta t = -0.7$ ps spectrum does not indicate the presence of a new chemical species but rather a coherent interaction, as observed and predicted by Roke[13] for CO on Ru{0001}. This feature is further discussed below. The theoretical spectra appear somewhat broader at their base than the experimental spectra, and are found to be less Lorentzian in profile. This is due to the fact that the polarization decay, which is Fourier transformed to obtain the spectra, can never be perfectly exponential in form due to the superposition of the finite temporal width Gaussian form laser field at the initial stages of the decay. It would seem therefore that we have overestimated the temporal width of this field.

Plots of the experimental and theoretical center frequencies are shown in Figure 2.

Discussion

Before discussing the time-resolved SF spectra, we turn our attention to the static temperature dependence of the C−O stretch frequency (Figure 3). As mentioned in the Introduction, this is commonly believed to be due to anharmonic coupling of the C−O stretch to lower frequency modes such as the frustrated translation (47 cm^{-1} for CO/Ru{0001}[20]), the frustrated rotation (412 cm^{-1} for CO/Ru{0001}[7]), or the adsorbate−metal stretch (453 cm^{-1} for CO/Ru{10$\bar{1}$0}[1]). Excitation of a low-frequency mode modulates the C−O stretch, which renders both the frequency and the line width temperature-dependent (so-called vibrational dephasing[8]). The low-frequency mode itself is typically damped strongly by coupling to substrate phonons or by creation of electron−hole pairs. The only mode that can be excluded a priori is the adsorbate−metal stretch, as this would lead to a weakening of the CO−Ru bond and a blue shift of the C−O stretch frequency, unlike the observed red shift with increasing temperature. This is also discussed by Bonn et al.[3] in connection with their time-resolved SF spectra.

The static temperature dependence of the C−O stretch has been measured for a wide range of surfaces, and in particular for the Ru{0001} surface at 0.33 ML coverage. Our data at a coverage of 0.9 ML show a temperature change of the frequency that is 30% stronger than on the close-packed surface.[7] On Ru{0001} the line width changes by less than 1 cm^{-1} between 50 and 300 K. Over the temperature range of 100−260 K we do not detect any changes in width within our experimental error of about 1 cm^{-1}.

There are no data available for the low-frequency modes of CO adsorbed on Ru{10$\bar{1}$0} other than for the metal−CO stretch, but it is possible to make an educated guess by comparison to CO adsorbed on platinum. On the Pt{111} surface at 0.25 ML coverage the frustrated translation mode has been measured[21] as 56 cm^{-1}. On Pt{110}, where CO adsorbs in on-top positions on the ridges, the frustrated translation across the ridge is[22] 45 cm^{-1}, while along the ridge the frequency is 53 cm^{-1} for the (1×1) surface and 58 cm^{-1} for the (1×2) surface.

A simplified model[23] gives analytical expressions for the changes in temperature and width (but ignores lateral interactions):

$$\Delta\Omega(T) = (\delta\omega)n(\omega_1, T) \tag{11}$$

$$\Gamma(T) = n(\omega_1,T)[n(\omega_1,T) + 1]\frac{(\delta\omega)^2}{\eta} \tag{12}$$

$$n(\omega_1,T) = \frac{1}{e^{\hbar\omega_1/kT} - 1} \tag{13}$$

where $\Delta\Omega(T)$ is the change in stretch frequency (as a function of temperature), $\Gamma(T)$ is the half line width of this mode, ω_1 is the low-frequency mode, $\delta\omega$ is the change in stretch frequency when the low-frequency mode is excited, η is the damping rate of the low-frequency mode, and $n(\omega_1,T)$ is the Boltzmann occupation factor of that mode.

From eq 11 one can estimate that a 20% lowering of ω_1 (as in the example of Pt) leads to an overall increase in $\Delta\Omega$ of 23% over the 100−250 K range. If we assume a similar change in the frustrated translation for Ru{0001} and Ru{10$\bar{1}$0}, then $\delta\omega$ would have to increase by 7% to reproduce the stronger temperature dependence on Ru{10$\bar{1}$0}; that is, from the −3 cm^{-1} determined[7] for Ru{0001} we would deduce a value of −3.2 cm^{-1} for Ru{10$\bar{1}$0}. Using a similar argument for the damping constant, we would expect a value similar to that of the closed-packed surface, 4.5 cm^{-1}.

Using the elastic continuum model,[24] it is possible to calculate the phonon contribution to the damping of the frustrated translation mode, which results in a damping constant of 0.2 cm^{-1}. We therefore come to the same conclusion as Jakob and Persson, namely, that the damping of the frustrated translation mode may be mainly electronic in character. This would suggest coupling to the electronic heat bath.

From our simulation of the pump/probe data (Figure 2) it is clear that there is very little difference between fast thermal coupling to the ruthenium phonons alone and additional coupling to the electrons with time constants above about 5 ps. This is mainly due to the vibrational dephasing (T_2), which "washes out" the faster rise in temperature. The reason for the ambiguity is the strong electron−phonon coupling constant for Ru, which at 1.85×10^{18} W m^{-3} K^{-1} is very similar to the constant for Pt (1.8×10^{18} W m^{-3} K^{-1}) but about 20 times larger than that for Cu. Such a strong coupling results in an equilibration time between electrons and phonons very similar to T_2.

An argument for pure phonon coupling (as used by Bonn et al.[3,13]) would have to come from supporting measurements (laser-induced desorption in the case of CO/Ru{0001}[12]) instead. Very fast coupling to the electrons or any fast, i.e., <1 ps, changes in the C−O frequency on the other hand would leave a significant mark on the SF spectra, as we shall now see.

Spectra produced from much increased electron−adsorbate thermal coupling have multiple side peaks around $\Delta t < 0$ and $\Delta t \simeq 0$ which are not observed by experiment. As an extreme

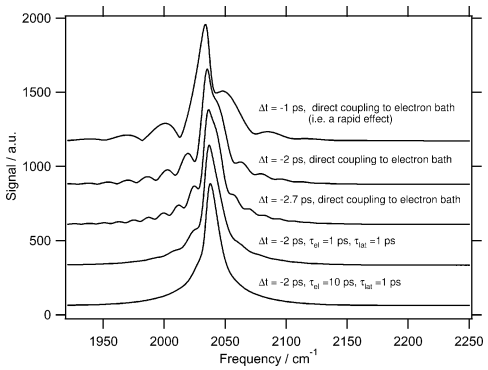

Figure 5. Comparison between theoretical SF spectra (pump *after* probe) with some thermal coupling of the adsorbate to the lattice and with all thermal effects due to hot electrons, the latter being shown for three different pump/probe delays, Δt.

case, if the adsorbate temperature is set equal to the electronic temperature (assuming that the empirical linear frequency−temperature relationship in eq 6 still holds at high temperature), then spectra such as those shown in Figure 5 are obtained, with many side oscillations. These oscillations are of a time period ($\Delta t = 2\pi/\Delta\omega$) equal to the pump/probe delay. This is also true (but less pronounced) when there is coupling to the lattice, and for the model given by Roke[13] for CO/Ru{0001}. The increased amplitude of these oscillations with increasing electronic coupling could be used as an indication of the degree of thermal electronic coupling from future experimental spectra. Although we measured no change in T_2 with respect to temperature for CO/Ru{10$\bar{1}$0}, if such a change is artificially introduced into the model, the effect is to increase the height of the side peaks relative to the main peak. This could explain the large side peaks seen by Roke et al.[13]

If instead a blue shift occurs around $\Delta t \approx 0$, then the theoretical spectra are mirror images about the center frequency. Again, this could be used to quickly interpret future pump/probe spectra for $\Delta t < 0$ and $\Delta t \simeq 0$ on the basis of whether any asymmetry is toward lower (red-shifted) or higher (blue-shifted) frequencies.

The only real difference between the parameters applied to the Bloch equations in the case of electronic thermal coupling alone is the rapidity of the frequency shift, so we suggest that other rapid causes of frequency shift, such as pump laser induced *direct* electronic interactions with the adsorbate, would cause such oscillations in the spectra.

In our case we can rule out direct electronic excitation of the CO, as the pump wavelength of 800 nm is too far in the red. For the saturation coverage of CO on Ru{0001} the CO $2\pi^*$ orbital was found[25] at 4.9 eV above the Fermi energy, more than 3 times higher than our photon energy. Moreover, if our system had an electronic excitation mechanism whereby the C−O stretch frequency was changed on the ultrafast time scale of an electronic excitation, then from the theoretical spectra presented in this paper, we should have observed significant spectral features (oscillations) in our experimental SF spectra.

Conclusions

We observed a transient red shift of the C−O stretch frequency on Ru{10$\bar{1}$0}, when pumped by a femtosecond 800 nm pulse. Using the Bloch equations, this transient shift can be modeled on the basis of the temperature dependence of the C−O stretch, caused by anharmonic coupling to a low-frequency adsorbate mode, which is either the frustrated translation or the frustrated rotation. While we cannot tell from the time-resolved SF data whether this mode in turn thermally couples to the ruthenium phonons exclusively or to the electrons on a time scale of 5−10 ps, we can conclude that the effect is thermal rather than due to direct electronic excitation, by comparison of the line shape with theoretical spectra when such a rapid effect is considered. A reflection−absorption infrared spectroscopy (RAIRS) study of the low-frequency adsorbate modes of CO on Ru{10$\bar{1}$0} and their temperature dependence could clarify whether the damping mechanism is via thermal phonon or electron coupling.

Acknowledgment. We are grateful to the EPSRC and CERC3 for equipment funding. J.P.R.S. and H.A. thank the EPSRC for personal funding, and in addition J.P.R.S. thanks Johnson Matthey plc and the Newton Trust. We thank Sylvie Roke for many useful discussions.

References and Notes

(1) Lauth, G.; Solomun, T.; Hirschwald, W.; Christmann, K. *Surf. Sci.* **1989**, *210* (1, 2), 201−224.
(2) Rotaris, G.; Baraldi, A.; Comelli, G.; Kiskinova, M.; Rosei, R. *Surf. Sci.* **1996**, *359* (1−3), 1−9.
(3) Bonn, M.; Hess, C.; Funk, S.; Miners, J. H.; Persson, B. N. J.; Wolf, M.; Ertl, G. *Phys. Rev. Lett.* **2000**, *84* (20), 4653−4656.
(4) Beckerle, J. D.; Casassa, M. P.; Cavanagh, R. R.; Heilweil, E. J.; Stephenson, J. C. *Phys. Rev. Lett.* **1990**, *64* (17), 2090−2093.
(5) Germer, T. A.; Stephenson, J. C.; Heilweil, E. J.; Cavanagh, R. R. *Phys. Rev. Lett.* **1993**, *71* (20), 3327−3330.
(6) Culver, J. P.; Li, M.; Jahn, L. G.; Hochstrasser, R. M.; Yodh, A. G. *Chem. Phys. Lett.* **1993**, *214* (5), 431−437.
(7) Jakob, P.; Persson, B. N. J. *Phys. Rev. B* **1997**, *56* (16), 10644−10650.
(8) Persson, B. N. J.; Hoffmann, F. M.; Ryberg, R. *Phys. Rev. B* **1986**, *34* (4), 2266−2283.
(9) Tully, J. *Annu. Rev. Phys. Chem.* **2000**, *51*, 153−178.
(10) Germer, T. A.; Stephenson, J. C.; Heilweil, E. J.; Cavanagh, R. R. *J. Chem. Phys.* **1993**, *98* (12), 9986−9994.
(11) Hunt, J. H.; Guyot-Sionnest, P.; Shen, Y. R. *Chem. Phys. Lett.* **1987**, *133* (3), 189−192.
(12) Funk, S.; Bonn, M.; Denzler, D. N.; Hess, C.; Wolf, M.; Ertl, G. *J. Chem. Phys.* **2000**, *112* (22), 9888−9897.
(13) Roke, S.; Kleyn, A. W.; Bonn, M. *J. Phys. Chem. A* **2001**, *105* (10), 1683−1686.
(14) Arnolds, H.; Symonds, J. P. R.; Zhang, V. L.; King, D. A. *Rev. Sci. Instrum.* **2003**, *74* (9), 3943−3946.
(15) Symonds, J. P. R.; Arnolds, H.; Zhang, V. L.; Fukutani, K.; King, D. A. *J. Chem. Phys.*, **2004**, *120*, 7158−7164.
(16) Shen, Y. R. *The Principles of Nonlinear Optics*; John Wiley and Sons: New York, 1984.
(17) Anisimov, S. I.; Kapeliovich, B. L.; Perel′man, T. L. *Sov. Phys. JETP* **1974**, *39*, 375.
(18) NAG Fortran library routine D03PF Mark 18.
(19) Boyd, R. W. *Nonlinear Optics*, 2nd ed.; Academic Press: San Diego, 2003.
(20) Braun, J.; Kostov, K. L.; Witte, G.; Wöll, C. *J. Chem. Phys.* **1996**, *106* (19), 8262−8273.
(21) Graham, A. P. *J. Chem. Phys.* **1998**, *109* (21), 9583−9586.
(22) Ge, Q.; King, D. A. *J. Chem. Phys.* **1999**, *111* (21), 9461−9464.
(23) Persson, B. N. J.; Ryberg, R. *Phys. Rev. B* **1989**, *40* (15), 10273−10281.
(24) Persson, B. N. J.; Ryberg, R. *Phys. Rev. B* **1985**, *32* (6), 3586−3596.
(25) Benndorf, C.; Bertel, E.; Dose, V.; Jacob, W.; Memmel, N.; Rogozik, J. *Surf. Sci.* **1987**, *191* (3), 455−465.